

# A DETERMINATION OF THE ATMOSPHERIC GAMMA-RAY SPECTRUM BETWEEN 10 AND 100 MEV MADE AT HIGH GEOMAGNETIC CUT-OFF RIGIDITIES

I. N. Azcárate<sup>1</sup>

Instituto Argentino de Radioastronomía, Argentina

*Received 1999 October 18; accepted 2000 March 16*

## RESUMEN

Se reportan los resultados de dos experimentos llevados a cabo con un detector plástico omnidireccional sensible a radiación gama de relativamente alta energía y que fue transportado en las dos ocasiones por un globo estratosférico. Los vuelos ocurrieron el 18 de noviembre de 1990 y el 24 de febrero de 1992, en lugares de rigideces de corte geomagnético de 11.1 y 11.5 GV, respectivamente. Para este detector omnidireccional y para energías mayores que algunos MeV, la mayor parte de los fotones detectados son rayos gama secundarios, producidos por interacciones de los rayos cósmicos cargados con la atmósfera. Para obtener el espectro de rayos  $\gamma$  incidente a partir del espectro de altura de pulsos observado en el detector, se calcula la función respuesta en forma numérica con algunas hipótesis simplificadoras. Usando esta función de respuesta, se obtiene un flujo diferencial de fotones  $dJ/dE = E^{-1.2 \pm 0.2}$  en fotones  $\text{cm}^{-2} \text{s}^{-1} \text{MeV}^{-1}$ , promediado sobre todos los ángulos cenitales, que corresponde a la radiación gama atmosférica a  $5 \text{ g cm}^{-2}$  de profundidad atmosférica y en el intervalo de energías de 10 a 100 MeV. Este flujo obtenido resulta ser compatible con los resultados de otras observaciones hechas con diferentes tipos de detectores y a diferentes rigideces de corte geomagnéticos.

## ABSTRACT

The results of two experiments carried out with a large volume balloon-borne omnidirectional plastic scintillator sensitive to high-energy gamma-radiation are reported here. The two flights were carried out on 18 November 1990 and 24 February 1992, at places of 11.1 and 11.5 GV geomagnetic cut-off rigidities, respectively. For an omnidirectional detector and for energies greater than several MeV, most of the detected photons are secondary  $\gamma$ -rays produced through interactions of the charged cosmic rays with the atmosphere. To unfold the observed pulse height spectrum and obtain the incident  $\gamma$ -ray spectrum, the detector response function is calculated numerically with some simplifying assumptions. By using this response function, a differential flux  $dJ/dE = E^{-1.2 \pm 0.2}$  photons  $\text{cm}^{-2} \text{s}^{-1} \text{MeV}^{-1}$ , averaged over all zenith angles, is estimated for the atmospheric  $\gamma$ -radiation, at an atmospheric depth of  $5 \text{ g cm}^{-2}$ , in the 10–100 MeV energy range. This flux turns out to be compatible with other observations made with different types of detectors and at different geomagnetic cut-offs.

**Key Words:** ATMOSPHERIC EFFECTS — BALLOONS — GAMMA RAYS: OBSERVATIONS

## 1. INTRODUCTION

Although the X-or  $\gamma$ -rays observations, made with instruments transported by stratospheric bal-

<sup>1</sup>Member of the Carrera del Investigador Científico y Tecnológico of CONICET, Argentina.

loons, are related to the detection of this radiation from the Sun and other celestial sources, the study of the atmospheric background, originated by means of interactions between cosmic rays and air nuclei, their source function and propagation, may still be

considered of interest. As an example, in relation to the Pierre Auger Project, the Monte Carlo computations that are carried out to estimate the production of secondary particles and photons caused by interactions of primary charged cosmic rays, with an incidence in the atmosphere, may benefit from the measurement of atmospheric  $\gamma$ -ray spectra. Inorganic scintillators (Cs I or Na I) either uncollimated or with active or passive collimation (Haymes et al. 1969; Peterson, Schwartz, & Ling 1973; Azcárate 1999) have been used to observe this type of radiation in the energy range up to 20 MeV.

Schoenfelder, Graser, & Daugherty (1977), Schoenfelder, Graml, & Penningsfeld (1980), and Ryan et al. (1977; 1979) have made  $\gamma$ -radiation measurements, covering the energy range 1–25 MeV, by using double Compton telescopes.

Spark chambers (Staib, Frye, & Zych 1974; Fichtel, Kniffen, & Ogelman 1969; Kniffen et al. 1978; Thompson, Simpson, & Ozel 1981) or combinations of spark chambers with other detectors, such as nuclear emulsions (Kinzer, Share, & Seeman 1974) have been used for energies higher than some tens of MeV. Both the spark chamber and the double Compton telescope are directional detectors, and most of the intensity and spectral measurements refer to the vertical direction.

When an inorganic scintillator is used, the derivation of the incident spectrum from the observed pulse-height spectrum, requires a rather complex procedure, and this is why some of the results presented in the literature are simply the observed energy-loss spectra, which sometimes make the comparison between them rather difficult. Martin (1974), has used the Monte Carlo method to obtain a response function.

Klumpar et al. (1973) have measured the  $\gamma$ -ray spectra with a small liquid scintillator (NE-213) in the 1–10 MeV energy range. By using this kind of detector, they are able to derive, under some simplifying assumptions, the incident atmospheric  $\gamma$ -ray spectrum.

The results of observations made with a large volume balloon borne plastic scintillator, used as a high energy  $\gamma$ -ray omnidirectional detector ( $E_\gamma \geq 4.5$  MeV) are hereby reported. The charged particles that, otherwise, would contribute to the pulse height spectrum, are efficiently rejected by an almost  $4\pi$  anti-coincidence shielding.

The plastic scintillator is equally sensitive to high energy gamma rays and fast neutrons of at least several MeV. However, several observations have shown (White et al. 1973; Kanbach, Reppin, & Schoen-

felder 1974; Preszler, Simnett, & White 1974; Bhatt 1976) that the fluxes of atmospheric neutrons of some tens of MeV are several times lower than the fluxes of atmospheric gamma rays at equivalent electron energies. For that reason, in what follows, the hypothesis is made that the observed pulse spectra are mainly due to high-energy gamma rays. As will be shown below, this hypothesis is supported by the good agreement found between the observed and calculated pulse height spectra.

Due to the kind of interactions that produce the electron pulses, the energy range involved, the composition (mostly H and C atoms) and dimensions of the plastic scintillator, it was possible to obtain a response function to an assumed incident  $\gamma$ -ray spectrum, by using an approach rather similar to that of Klumpar et al. (1973), and without using elaborate calculation procedures. This is a comparative advantage of this large detector.

In the plastic scintillator, an instrumental  $\gamma$ -ray background due to neutrons interacting with C nuclei, is expected (Carter et al. 1977), but the energies of the  $\gamma$ -rays produced are below the threshold of the experiment reported here. The interaction between fast neutrons and C nuclei can produce  $\alpha$  particles and recoil C nuclei, but most of the light pulses produced by the ionizing products are (in the energy range considered in this paper) below the threshold of the experiment. On the contrary, recoil protons resulting from elastic interactions between fast high-energy neutrons and H nuclei in the detector certainly contribute to the energy-loss spectrum but, due to the relative abundance of these neutrons and gamma rays of equivalent electron energies, to ignore them does not introduce a significant error. In the next section, a short description of the detector system is given.

## 2. THE DETECTOR SYSTEM

The detector system was composed in its central part by a large volume plastic scintillator of parallelepipedal shape ( $16 \times 16 \times 24$  cm<sup>3</sup>) coupled through a light pipe to a 13 cm diameter phototube. This detector was surrounded by an almost  $4\pi$  plastic scintillator shielding, about 1 cm thick, which was used to remove electronically from the spectral analysis the events generated by charged particles that pass throughout both the central and the shielding plastics. The pulses in the external scintillator, commonly called “veto” pulses, were viewed by four 5.1 cm-diameter phototubes.

The geometric factor for the central detector was 3217 cm<sup>-2</sup> ster, for isotropic radiation incident

from one hemisphere, and its mean projected area 512 cm<sup>2</sup>. The low-energy threshold for detection of pulses produced on the central scintillator was set at 4.5 MeV of equivalent electron energy, which corresponds to about 10 MeV recoil protons.

The pulse height versus energy relationship did not depart from linearity by more than about 10%, up to at least 50 MeV of deposited energy, according to tests made at the laboratory. The rejection efficiency of the veto system was about 99%.

### 3. DETECTOR RESPONSE TO $\gamma$ RADIATION

Due to the composition of the central scintillator, which consists almost entirely of hydrogen and carbon atoms of equal numerical density, high-energy  $\gamma$ -radiation is mainly detected through the Compton process and pair creation. In the two cases, the resulting electrons produce the light pulses that excite the phototube. By knowing the response function, it is possible to obtain the incident  $\gamma$ -ray spectrum by unfolding the observed pulse-height spectrum. The response function was calculated with the following simplifying assumptions:

i) it is assumed that the photons are incident perpendicularly on a slab of the main scintillator with thickness  $L$ , followed by a second layer of scintillator to simulate the veto action.

ii) The energies involved and the large attenuation lengths in the plastic scintillator make it possible to neglect a second interaction of the secondary Compton photon.

iii) It is assumed that the electrons resulting from the interaction follow the direction of the incident photon, which is certainly valid for the highest energies considered here.

If  $(dN/dT)dT$  stands for the number of pulses corresponding to electrons (or electron-positron pairs) with total kinetic energies between  $T$  and  $T+dT$ ;  $J(E)$  the incident differential  $\gamma$ -ray spectrum, and  $\rho(E,T)$  the response function, we will have in general the relationship

$$dN/dT = \int_{E-T}^{\infty} \rho(E,T) \times J(E) dE \quad (1)$$

Assuming that  $J(E)$  is given by a power-law  $AE^{-\alpha}$ , considering the electron production through Compton and pair-creation processes, and integrating this production for different depths within the slab, the following formula is derived

$$dN(T)/dT = INTC + INTP \quad (2)$$

where

$$INTC = \int_{E_0}^{\infty} 1/\sigma_c(E) \times d\sigma_c(E,T)/dT \times \sigma_c(E)/\sigma_t(E) \times (1 - e^{-n\sigma_t(E)[L-R(T)]}) \times AE^{-\alpha} dE \quad (3)$$

and

$$INTP = A(T + 1.022)^{-\alpha} \times \sigma_p(E)/\sigma_{T(E)} \times [(2T_2/T - 1) - 2/T \int_{T/2}^{T_2} e^{-n\sigma_t(E)[L-R(T')]} dT'] \quad (4)$$

where  $INTC$  allows for the Compton effect and  $INTP$  for pair creation.  $d\sigma_c(E,T)/dT$  is the differential Compton cross section as given by the Klein-Nishina formula and  $\sigma_c(E)$  the corresponding total cross section,  $\sigma_p(E)$  is the total pair creation cross-section,  $n$  is the numerical density of the material,  $\sigma_t(E) = \sigma_c(E) + \sigma_p(E)$  is the total cross-section for the two processes. The integration limits are given by:  $E_0 = (T/2) (1 + \sqrt{1 + 1.022/T})$ ,  $T_2 = T$  if  $T \leq T^*$  and  $T_2 = T^*$  if  $T > T^*$ , being  $R(T^*) = L$ . To derive  $INTP$ , the differential cross-section for pair production was approximated by a rectangular function (between  $T^+ = 0$  and  $T^+ = T$ ). That function was obtained by considering that

$$\int_0^T d\sigma_p/dT^{\pm} \times dT^{\pm} = \sigma_p(E) \quad (5)$$

where  $T^-$  and  $T^+$  are the energies of the electron and positron resulting from a pair creation interaction, respectively, and we have taken as an average value

$$d\sigma_p/dT^{\pm} = T^{-1} d\sigma_p(E) \quad (6)$$

where  $T = T^+ + T^-$ .

In both terms, the factor within brackets, allows for the integral self-gating effect. By using this expression of the response function, the resulting energy-loss spectra have been calculated for various incident  $\gamma$ -ray spectra, assuming they are given by a power law, and taking as thickness of the slab  $L = 16$  cm and  $L = 24$  cm, corresponding to the main dimensions of the scintillator. The integration was made numerically and incident  $\gamma$ -ray energies up to 100 MeV were considered.

The general form of the calculated energy-loss spectra is given by a power law in its low-energy portion, up to about 30 MeV, and become progressively steeper, due to the self-gating, at higher energies

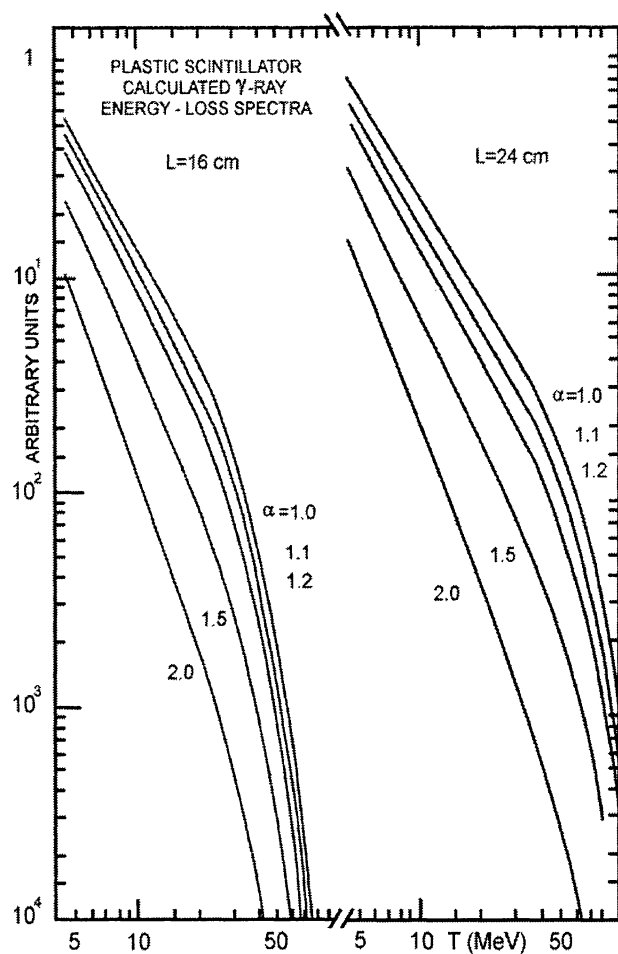


Fig. 1.  $\gamma$ -ray energy-loss spectra, calculated for a power-law ( $AE^{-\alpha}$ )  $\gamma$ -ray incident spectrum for various values of  $\alpha$ , and for  $L = 16$  cm and  $L = 24$  cm.

(see Figure 1). As will be shown below, this general form agrees with that corresponding to the observed energy-loss spectra in the atmosphere. For instance, in Figure 2 the calculated spectrum for  $\alpha = 1.2$  and  $L = 16$  cm, and the observed spectrum at a depth of  $9.5 \text{ g cm}^{-2}$  in one of the flights are shown.

The agreement found in the general form of the calculated and observed spectra would indicate the validity of the assumptions made to compute the response function. However, the excess of observed pulses at high energies results mainly from the departure of the real case from the simplifying hypothesis *i*) normal incidence on an uniform slab. The computation of the response function could be improved by considering the angular distribution of the incident radiation and the actual shape of the detector. Not taking these factors into account is the main cause

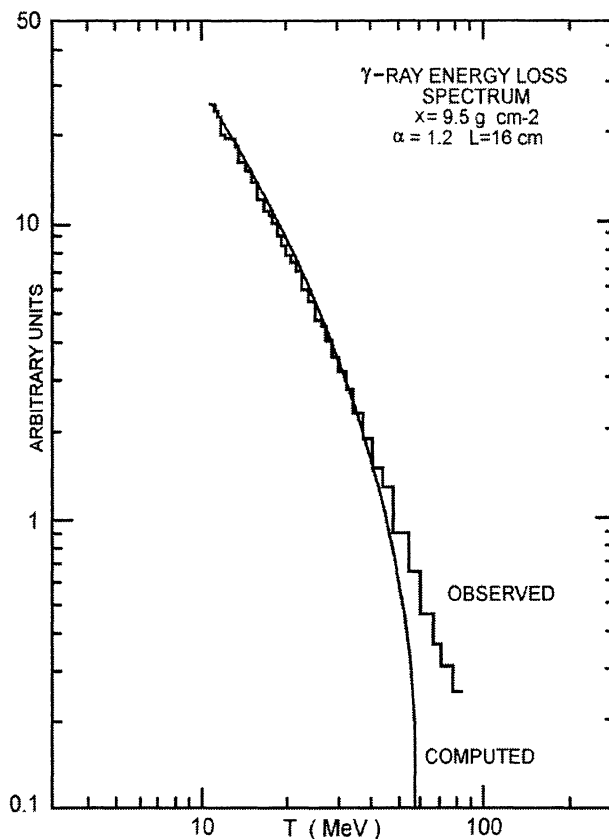


Fig. 2. Calculated  $\gamma$ -ray energy-loss spectrum for  $L = 16$  cm and  $\alpha = 1.2$  compared with the observed spectrum at  $9.5 \text{ g cm}^{-2}$  residual atmosphere.

in the uncertainty in the derived exponent for the gamma-ray spectrum. On this respect, it is worthwhile to mention that a Monte Carlo simulation for isotropic gamma-ray with an incidence on a cylindrical plastic detector of dimensions comparable to that considered here, fits better, also for  $\alpha = 1.2$ , the high-energy portion of the observational points shown in Figure 2 (Gruber 1980, personal communication).

The detection efficiency for gamma-rays of the central plastic scintillator was also computed with the same main approximations made for the calculation of the response function. For a detection low-energy threshold  $T_b$  of 4.5 MeV and neglecting the self-gating effect, the computed efficiency remains above 20 and 30% for  $L = 16$  cm and  $L = 24$  cm, respectively. The self-gating effect reduces the value of the efficiency for energies larger than some tens of MeV greatly. However, also for  $T_b = 4.5$  MeV and  $L = 16$  cm, the efficiency peaks around 20%, and is above 10% for gamma-rays up to 25 MeV and simi-



larly for  $L = 24$  cm it peaks around 30% and is above 10% for gamma-rays up to 55 MeV.

#### 4. EXPERIMENTS AND RESULTS

Two experiments were made with stratospheric balloons, that were launched on 18 November 1990, from Paraná, Argentina (11.1 GV geomagnetic cut-off) and 24 February 1992, from Reconquista, Argentina (11.5 GV geomagnetic cut-off). The balloons reached ceiling altitudes of  $5 \text{ g cm}^{-2}$  and  $9.5 \text{ g cm}^{-2}$ , respectively.

In both flights the gamma-ray low-energy threshold was set at about 4.5 MeV. However, to be sure that the spectra are clean of most of the instrumental background arising at the lowest energies, they are given for energies above 10 MeV. On the other hand, because of the self-gating effect, the  $\gamma$ -rays had a nominal upper threshold of about 200 MeV, given by the maximum possible electron pathlength within the central crystal.

The observed pulse height spectra were obtained by taking samples of 10 min during the ascent of the balloon, and several samples of more than 1 hr each were recorded at floating altitude. The shape of the energy-loss spectra observed during the two flights agree quite well, being compatible with that expected from the computations for a power-law incident spectrum.

In Figure 3 several energy-loss spectra observed at different atmospheric depths are shown. The result is that in the 10–30 MeV energy range, where these observed spectra are fitted by a power-law  $dN/dT = BT^{-\beta}$ , the values of the exponent  $\beta$ , which range between 1.8 and 1.9, do not change sensibly with depth. This is valid between 5 and about  $200 \text{ g cm}^{-2}$ , that is even below the Pfotzer maximum for the integral counting rate observed at about  $120 \text{ g cm}^{-2}$ . At higher energies, the observed spectra near ceiling altitude, in both flights, show a relatively larger abundance of high-energy photons than observed at greater depths. This appears compatible, at least qualitatively, with the general energy degradation of high-energy photons when they penetrate deeper in the atmosphere.

By using the response function as given by equations (3) and (4), we can derive, for instance, from the observed spectrum at  $5 \text{ g cm}^{-2}$ , that the law for the atmospheric  $\gamma$ -ray differential flux averaged over all zenith angles is of the form

$$dJ/dE = (0.33 \pm 0.1) E^{-1.2 \pm 0.2} \text{ photons cm}^{-2} \text{ s}^{-1} \text{ MeV}^{-1}. \quad (7)$$

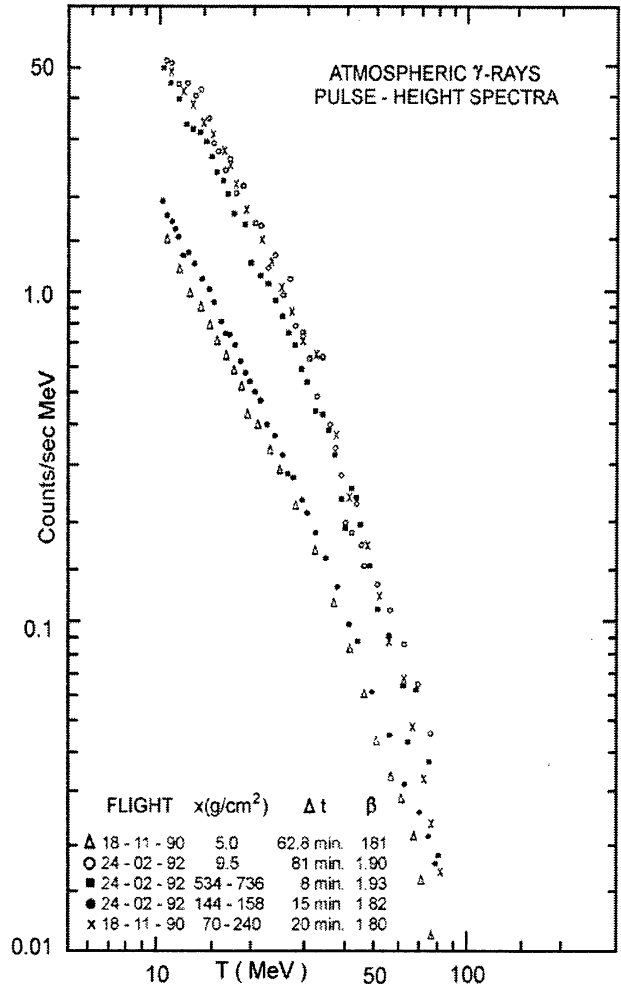


Fig. 3. Observed pulse-height spectra, registered at different atmospheric depths during the flights of 18 November 1990 and 24 February 1992.

This energy distribution is estimated to be valid up to about 100 MeV.

The values of the coefficient  $A$  and the exponent  $\alpha$  for this law were obtained using  $L = 16$  cm in the response function. This  $L$  corresponds to the detector transversal dimension-flown with its longer axis along the vertical, and is close to the most probable pathlength for photons arriving isotropically on it, and even closer to such pathlength for an angle distribution peaked near the horizon.

The uncertainty quoted for  $\alpha$  (and the corresponding  $A$ ) is simply the range of its values that result using either  $L = 16$  or  $L = 24$  cm to fit the power-law portion of all the spectra observed between 5 and  $200 \text{ g cm}^{-2}$  depth, and reflects its dependence on  $L$ . For instance, for  $L = 24$  cm,  $\alpha = -1.4$  reproduces

equally well the slope of the observed spectra. Factor  $A$ , which is obtained normalizing the computed and observed energy-loss spectrum, depends strongly on  $\alpha$  (as  $\alpha^{-10/3}$ ).

For a more accurate spectral determination, the direction and point of incidence on the detector of the  $\gamma$ -radiation should be considered, since the path-length  $L$  within it, depends on them. The lack of inclusion of the real angular distribution and the real detector shape, which would have made the computation much more complex, are the main cause of uncertainty in the determination of the incident photon spectrum.

### 5. COMPARISON WITH OTHER MEASUREMENTS

The photons resulting from primary and secondary cosmic-ray interactions with the air nuclei constitute the photon component of pure atmospheric origin. To this component are added the energy degraded secondary photons resulting from Compton and pair-creation of the primary  $\gamma$ -rays themselves.

On the other hand, for omnidirectional detectors that integrate the contribution of  $\gamma$ -rays arriving from all angles from both hemispheres, it is known that most of the detected photons are “purely atmospheric”.

This is also the case for the nearly omnidirectional system considered here, as shown by the very similar behavior, near the top of the atmosphere, of the growth curves for the integral counting rates of the central scintillator ( $E_\gamma > 4.5$  MeV) and the shielding scintillator that detects charged particles and photons with energies above a few tens of keV. Besides, a quite similar growth curve is observed in another measurement carried out at the same geomagnetic cut-off made with counters sensitive mostly to charged particles.

Ling (1975), making use of the source function concept, has calculated the intensity-depth relationship for unidirectional  $\gamma$ -radiation up to 10 MeV at different zenith angles. His results show, for the downward vertical intensity, a predominance of the diffuse cosmic component at atmospheric depths less than  $10 \text{ g cm}^{-2}$ . On the contrary, the diffuse component is not relevant in the horizontal and upward vertical total intensities.

For these reasons, in what follows, this spectral determination at high geomagnetic cut-off is compared with other measurements of the atmospheric  $\gamma$ -ray component in energy ranges at and around the energy range of this experiment. The best estimate

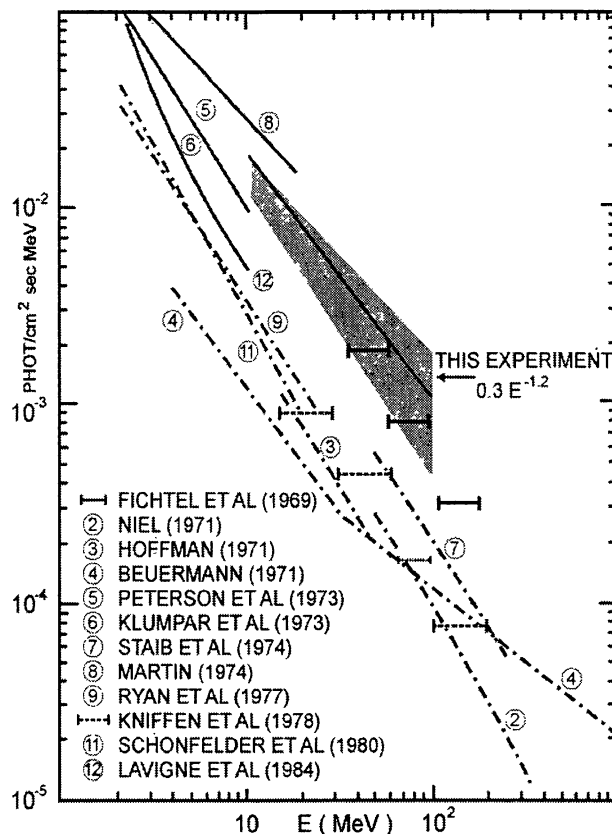


Fig. 4. Comparison of several determinations of the atmospheric  $\gamma$ -ray spectrum, reduced to an atmospheric depth of  $3 \text{ g cm}^{-2}$  and  $11.5 \text{ GV}$  geomagnetic cut-off. The limits of the dotted zone of uncertainty around the best estimation of the spectrum from the present experiments, represent the extreme limits of the differential flux that result assuming  $L = 16 \text{ cm}$  or  $L = 24 \text{ cm}$  in the computation of the response function.

of the incident  $\gamma$ -ray spectrum is shown in Figure 4, together with the limits given by the uncertainty in both  $A$  and  $\alpha$ .

Results of other spectral measurements of atmospheric  $\gamma$ -rays made by other authors are also shown, all reduced—including those of the experiment reported here—to  $3 \text{ g cm}^{-2}$  atmospheric depth. In all cases the omnidirectional flux is given, in photons  $\text{cm}^{-2} \text{ s}^{-1} \text{ MeV}^{-1}$ . To reduce the results to  $3 \text{ g cm}^{-2}$ , the extrapolation of the relationship intensity versus depth, obtained from the central detector counting rate is used. This relationship may be fitted, for atmospheric depths below  $15 \text{ g cm}^{-2}$ , by a power-law  $C \propto x^\nu$  (see below), where  $\nu$  is  $0.28$  and  $x$  is the atmospheric depth. As most of the other measurements have been carried out at a geomagnetic

cut-off of 4.5 GV, a factor was applied to correct these results to 11.1 GV. The factor 0.57 used here, was estimated by Staib et al. (1974) from the results of their measurements of vertical  $\gamma$ -rays between 50 and 1000 MeV at 4.5 GV and 12 GV.

Three of the measurements shown here were made with omnidirectional detectors: Peterson et al. (1973) used a  $3'' \times 3''$  Na I scintillator in the 0.2–10 MeV energy range, Klumpar et al. (1973) used a  $4.65 \times 4.60$  cm liquid scintillator (NE-213) in the 1–10 MeV energy range, and Martin (1974) used a  $4'' \times 4''$  Na I scintillator in the 0.7–18 MeV energy range. The results presented by Peterson et al. are unfolded fluxes, given in counts  $\text{cm}^{-2} \text{s}^{-1} \text{MeV}^{-1}$ .

The other measurements considered here, were made with directional detectors (Fichtel et al. 1969; Hoffman 1971; Niel 1971; Staib et al. 1974; Ryan et al. 1977; Kniffen et al. 1978; Schoenfelder et al. 1980; Lavigne, Niel, & Vedrene 1984). However, Fichtel et al. give omnidirectional flux, integrating their directional measurements over all the zenith angles. For comparison with the other measurements I had to assume isotropic incidence and to obtain the omnidirectional flux, it was necessary to multiply by  $4\pi$ . As shown in Figure 4, the results of the experiments reported here best agree with Fichtel et al. measured between 30 and 300 MeV, and are compatible with other omnidirectional determinations at lower energies.

The absolute fluxes from the directional measurements and those resulting from Beuerman's (1971) theoretical calculations are systematical lower than the results of the experiments described in the present paper. This can be explained, on the one hand, by the fact that they refer essentially to vertical downward  $\gamma$ -ray intensities and, according to calculations and measurements of other authors (Thompson 1974; Schoenfelder et al. 1977; Graser & Schoenfelder 1977; Thompson et al. 1981), the well-known angular distribution of the  $\gamma$ -ray intensity near the top of the atmosphere shows a minimum for the downward vertical direction, and a maximum near the horizontal direction. On the other hand, the value of the mean projected area ( $512 \text{ cm}^2$ ), that it is used here to obtain the absolute flux is that of the parallelepipedical detector in an isotropic field of radiation, which is smaller than the value that would result for an angular distribution peaked along the horizon. Therefore, I estimate that a reduction by a factor of around two in its flux could be justified by this reason. This fact would improve the agreement with Fichtel's values.

The obtained omnidirectional differential energy

spectrum (within the intermediate energy range 10–100 MeV) is also flatter than those resulting from most of the energy spectra measured along the vertical direction at smaller and larger energies. However, it seems to be compatible with observations of downward moving medium energies atmospheric  $\gamma$ -rays made by Kinzer et al. (1974) and Kniffen et al. (1978) at almost the same geomagnetic cut-off and somewhat larger atmospheric depth. In this energy range two  $\gamma$ -ray production mechanisms compete in the atmosphere: bremsstrahlung and  $\pi^0$  decay, the former being more relevant at the low-energy portion of the range. On the other hand, the contribution of neutral pion decays, as suggested by the observations of Kinzer et al., dominates the higher energies, particularly at the high cut-off rigidity ( $\approx 11.5$  GV) of the measurement reported in this paper. This effect would thus explain the smaller exponent of the assumed power-law spectrum used to fit the observations in the whole energy range. Also the atmospheric  $\gamma$ -ray spectrum calculated for 10 GV cut-off by Daniel & Stephens (1974) over a wide range of energies shows a similar flattening in the intermediate energies.

From this discussion, I argue that the determination reported in this paper may be considered to be compatible with other measurements.

This research has been supported by grant PIP 0430/98 from the National Scientific and Technical Research Council (CONICET), from Argentina. I. N. Azcárate is a Member of the Carrera del Investigador Científico y Tecnológico of CONICET.

## REFERENCES

- Azcárate, I. N. 1999, BAAS, 31 No. 2, 722
- Beuerman, K. P. 1971, JGR, 76, 4291
- Bhatt, V.L. 1976, JGR, 81, 4603
- Carter, J., Dean, A. J., Manchanda, R. K., & Ramsden, D. 1977, Space Sci. Instr., 3, 123
- Daniel, R. R., & Stephens, S. A. 1974, Rev. Geophys. Space Phys., 12, 233
- Fichtel, C. E., Kniffen, D. A., & Ogelman, H. B. 1969, ApJ, 158, 193
- Graser, V. A., & Schoenfelder, V. 1977, JGR, 82, 1055
- Gruber, D. 1980, private communication
- Haymes, R. C., Glenn, S. W., Fishman, G. J., & Harneden, F. R. 1969, JGR, 74, 5792
- Hoffman, J. A. 1971, Smithsonian Astrophys. Obs. Spec. Report, 335
- Kanbach, G., Reppin, C., & Schoenfelder, V. 1974, JGR, 79, 5159
- Kinzer, R. L., Share, G. H., & Seeman, N. 1974, JGR, 79, 4567

- Klumpar, D. M., Lockwood, J. A., St Onge, R. N., & Friling, L. A. 1973, JGR, 78, 7959
- Kniffen, D. A., Bertsch, D. L., Morris, D. J., Palmeira, R. A. R., & Rao, K. R. 1978, ApJ, 225, 591
- Lavigne, J. M., Niel, M., & Vedrene, G. J. 1984, JGR, 89, 5636
- Ling, J. C. 1975, JGR, 80, 3241
- Martin, I. M. 1974, Determination des flux de photons gamma de basse energie dans l'atmosphere, Ph.D. thesis, Université Paul Sabatier de Toulouse, France
- Niel, M. 1971, Recherche en balloon de sources de rayonnement gamma cosmique d'energie superieure a 60 MeV, Ph.D. thesis, Université Paul Sabatier de Toulouse, France
- Peterson, L. E., Schwartz, D. A., & Ling, J. C. 1973, JGR, 78, 7942
- Preszler, A. M., Simnett, G. M., & White, R. S. 1974, JGR, 79, 17
- Ryan, J. M., Dayton, B., Moon, S. H., Wilson, R. B., Zych, A. D., & White, R. S. 1977, JGR, 82, 3593
- Ryan, J. M., Jennings, M. C., Radwin, M. D., Zych, A. D., & White, R. S. 1979, JGR, 84, 5279
- Schoenfelder, V., Graml, F., & Penningsfeld, F. P. 1980, ApJ, 240, 350
- Schoenfelder, V., Graser, U., & Daugherty, J. 1977, ApJ, 217, 306,
- Staib, J. A., Frye, G. M., & Zych, A. D. 1974, JGR, 79, 929
- Thompson, D. J. 1974, JGR, 79, 1309
- Thompson, D. J., Simpson, G. A., & Ozel, M. E. 1981, JGR, 86, 1265
- Thompson, M. N., & Taylor, J. M. 1965, Nucl. Instr. Meth., 37, 305
- White, R. S., Moon, S. H., Preszler, A. M., & Simnett, G. M. 1973, Space Res., 13, 683

Ismael N. Azcárate: Instituto Argentino de Radioastronomía, Casilla de Correo No. 5, (1894) Villa Elisa, Prov. de Buenos Aires, Argentina (azcarate@irma.iar.unlp.edu.ar).